buildings

MDPI

Article

Effect of Hybrid Carbon-Based Fillers on Electrical and Mechanical Performance of Strain-Hardening Cementitious Composites (SHCCs)

Liangliang Wei [1,2], Chenxi Xiao [1], Bixuan Yang [3], Shouwang Hu [1,2] and Yu Zheng [1,2,*]

[1] School of Environment and Civil Engineering, Dongguan University of Technology, Dongguan 523808, China; liangwei@dgut.edu.cn (L.W.); xcx@dgut.edu.cn (C.X.); shouwang.hu@dgut.edu.cn (S.H.)
[2] Guangdong Provincial Key Laboratory of Intelligent Disaster Prevention and Emergency Technologies for Urban Lifeline Engineering, Dongguan 523808, China
[3] Faculty of Science and Technology, University of Macau, Macao, China; yc57418@um.edu.mo
* Correspondence: zhengy@dgut.edu.cn

Abstract

Electrically conductive cement-based composites exhibit significant potential for a range of multifunctional applications. Nonetheless, the electrical and mechanical performance of ductile cement-based composites incorporating compound conductive additives has not been sufficiently explored. This study examines the effects of two distinct carbon-based fillers, namely carbon black and chopped carbon fibers, on strain-hardening cementitious composites (SHCC), and elucidates the synergistic mechanism of hybrid conductive fibers and fillers within SHCC. The findings indicate that a sufficiently high electrical conductivity can be achieved by incorporating 5 wt.% carbon black and 0.2–0.4 vol.% carbon fibers. The introduction of hybrid carbon-based fillers reduces the resistivity of SHCC by three orders of magnitude to less than 150 Ω·cm, surpassing the performance of composites with a single carbon-based filler. Furthermore, the incorporation of hybrid carbon-based fillers and fibers enhances the compressive and flexural strength of cementitious composites. Compared to the referenced PE-SHCC, the tensile strength and strain of SHCC with 5 wt.% carbon black and 0.4 vol.% carbon fibers increased by 37.3% and 82.6%, respectively. A hybrid efficiency index (HEI) is proposed to assess both electrical conductivity and mechanical properties of SHCC incorporating with carbon-based fillers. The study's findings offer an effective approach for utilizing hybrid carbon-based conductive fillers in the multifunctional applications of SHCC.

Keywords: carbon fiber; carbon black; electrical conductivity; PE fiber; SHCC

Academic Editors: Salvatore Verre and Giuseppina Uva

Received: 19 October 2025
Revised: 10 December 2025
Accepted: 6 January 2026
Published: 8 January 2026

1. Introduction

Cementitious composites are widely employed in various engineering structures due to their favorable mechanical properties, durability, and ease of fabrication. Recent advancements have facilitated the development of multifunctional cementitious composites that transcend traditional structural roles by incorporating additional capabilities [1–5]. While strength and stiffness remain their primary engineering functions, tailoring non-structural properties, such as electrical conductivity, magnetic response, and optical characteristics, imparts novel functionalities [6–10]. Among these potential enhancements, the introduction of electrical conductivity has attracted significant research interest due to its applicability in

 https://doi.org/10.3390/buildings16020267

areas such as self-sensing, electrothermal heating (e.g., for de-icing/snow-melting systems), and energy harvesting [8,11,12].

The construction industry is one of the major contributors to global resource consumption and carbon emissions. Therefore, developing more sustainable and resilient building materials is of vital importance in addressing climate change. Strain-hardening cementitious composites (SHCC) represent an advanced construction material characterized by their multiple cracking behavior and superior crack-width control under tensile stress [13–15]. This mechanical performance is attributable to the strategic incorporation of uniformly dispersed short discontinuous fibers within the cementitious matrix. Polymeric fiber reinforcements, particularly polyvinyl alcohol (PVA) and polyethylene (PE), are predominantly employed to generate significant bridging stress in SHCC systems [13–16]. A conductive network can maintain a significant portion of its integrity in the early stage of structural damage, thereby providing an ideal platform for more extensive and robust self-sensing functions. The stability of the conductive network within resilient SHCC is crucial for achieving effective long-term sensing and response. However, due to the non-conductive nature of PVA and PE fibers, conventional SHCC exhibits low electrical conductivity. This limitation can be addressed through the incorporation of conductive additives.

To achieve electrical functionality in cementitious composites, previous research has explored various conductive additives, including carbon fibers, carbon black (CB), multi-walled carbon nanotubes (MWCNTs), and metallic powders [17–19]. As a typical zero-dimensional (0D) carbon nanomaterial, CB is in a spherical shape or in clusters. The conductive network is mainly constructed through contact conduction forming a chain-like structure and quantum tunneling effect (i.e., electron transitions between particles in close proximity) [20]. Due to its point-contact nature, a relatively high additive content is required to form an effective conductive network (typically above 10 wt.% [21]). However, an excessively high content will introduce stress concentration points and defects, seriously compromising the strength and toughness of the composite material. Carbon fiber, characterized by its high aspect ratio and fibrous morphology, is a carbon-based material. It mainly forms a "bridging" effect through direct contact, establishing a macroscopic three-dimensional conductive network throughout the cement matrix [20]. With relatively small amounts of carbon fiber (typically around 0.8 vol.% [22]), a conductive network can be formed. The "bridging" effect of carbon fiber can effectively inhibit the expansion of microcracks, improving the toughness and tensile strength of the composite material. MWCNTs and graphene nanoplatelet (GNP) are in the form of tubes or sheets (2D), with an extremely high aspect ratio and specific surface area. They also form an efficient conductive network through contact conduction and quantum tunneling effects [20]. A very small amount of them can significantly enhance conductivity of the matrix. However, it is extremely difficult to achieve uniform dispersion in the cement matrix [23]. This is a significant technical challenge. Moreover, its large-scale application is severely limited by costs.

Zhu et al. [17] examined the electrical and fracture properties of hybrid fiber reinforced cementitious composites (HyFRCC) incorporating PE and carbon fibers. The findings indicate that the electrical resistivity of HyFRCC decreased by two orders of magnitude with the incorporation of 0.5 vol.% carbon fiber, and the fracture toughness of HyFRCC was also enhanced. Tian et al. [18] developed multifunctional SHCC using MWCNTs and carbon fibers, which demonstrated superior electrical conductivity, self-sensing performance, mechanical properties, and workability compared to copper-/aluminum-powder-modified counterparts. Generally, fibrous additives are preferred over particulate systems due to their significantly lower percolation threshold, which enables the formation of continuous conductive networks at a reduced volume fraction compared to powder-based additives.

On the other hand, powder-based conductive additives present distinct advantages over their fibrous counterparts. A significant limitation of fibrous additives is their propensity to agglomerate during mixing, which can potentially compromise the mechanical performance of the composite [24]. This agglomeration also impacts the formation of an effective conductive network. Regarding electrical conductivity, while the critical percolation threshold of any system is inherently characterized by an abrupt onset, previous studies have shown that powdered conductive additives often exhibit a relatively broader transition interval or more controllable resistivity change subsequent to percolation, allowing for finer tuning of conductivity [25]. This contrasts with conductive fibers, which typically manifest a steeper and more sensitive electrical response upon comparable concentration increments due to their efficient network formation at lower contents [26]. This sharp phase transition presents a challenge for precisely controlling the percolation network density through additive concentration, which is essential for multifunctional systems requiring sensitive and broad-range conductivity control. For piezoresistive materials, a progressive change in resistance via controlled network density with increasing additive concentration is crucial to achieve a broad sensing range and consistent performance. It is noteworthy that research on conductive cementitious composites has predominantly examined either fibrous or powder-based additives in isolation. While existing research has explored various combinations of conductive additives in cementitious composites [27–29], these studies often focus on specific aspects or material systems. A comprehensive investigation into the electrical and mechanical performance of ductile cementitious composites (SHCC) incorporating compound conductive additives, specifically designed to synergistically harness the distinct advantages of both powder-based and fibrous forms, remains less explored and consequently merits further investigation.

While conductive additives enhance the electrical properties of cementitious matrices, their incorporation presents significant challenges. SHCC typically has a lower water-binder ratio and a higher fiber volume fraction. This results in the high surface energy of nano-conductive fillers (such as carbon black) and carbon fibers with large aspect ratios being more prone to agglomeration during the mixing process. This, in turn, affects the uniform dispersion of these materials within the SHCC, hindering the formation of an effective conductive network and potentially having a negative impact on the original excellent mechanical properties of SHCC. Nalon et al. [30] demonstrated this by incorporating various carbon black (CB) nanoparticles, where composites containing 8% CB (by cement weight) exhibited a reduction in compressive strength from 17.6 MPa to 9.76 MPa. Similarly, excessive carbon fiber content promotes entanglement and agglomeration, further compromising the mechanical performance of conductive cementitious composites [31]. Consequently, there is a critical need to engineer cement-based materials capable of simultaneously fulfilling structural load-bearing requirements and providing reliable electrical conductivity.

In this study, an electrically conductive strain-hardening cementitious composite (SHCC) is developed by incorporating carbon black (CB), carbon fibers, and polyethylene (PE) fibers within a cementitious matrix. The objective is to achieve a synergistic enhancement of both electrical conductivity and mechanical performance. The electrical conductivity of the SHCC was characterized using the four-electrode voltammetry method, examining the influence of conductive additive dosage and curing age. Mechanical assessment included compressive strength, flexural strength, and, importantly, tensile performance. Then, both electrical conductivity and mechanical properties of conductive SHCC were evaluated by a proposed hybrid efficiency index. Furthermore, the study specifically investigates the synergistic conductive mechanisms between the fibrous carbon fibers and powder-based CB, exploring interactions arising from their distinct morphologies.

2. Materials and Methods

2.1. Materials

The complex Portland cement (P.C 42.5), silica fume (SF), and fine quartz sand were mixed with water to make a cementitious mortar matrix. The silica fume contained 96.7% SiO_2, and the average particle size of the fine sand was 30 µm. The nano carbon black dispersion liquid (CBDL) was supplied by a manufacturer (Runze Nano Technology Co., Ltd.) in Zhongshan, China. The nano carbon black (NCB) particles were dispersed in water using a specific polymeric dispersant, as illustrated in Figure 1a, where the solid content of NCB and the polymeric dispersant constituted 20 wt.% and 16 wt.% of the CBDL, respectively. The properties of NCB, which was the primary carbon-based filler, are detailed in Table 1. The diameter of the NCB particles was 15 nm (primary particle diameter provided by manufacturer), with a specific surface area of 65 m^2/g and a resistivity of 10 Ω·cm. It is noteworthy that the NCB existed in an agglomerated state rather than as individual particles in the dispersion liquid, due to the inherent characteristics of nanomaterials [32]. The distribution of NCB in the dispersion liquid is depicted in Figure 1b using a HORIBA laser scattering particle size distribution analyzer (HORIBA, Ltd., Kyoto, Japan). The mean size of NCB was 318 nm (agglomerated particle), and the 90% transmittance of cumulative quantity was 419 nm.

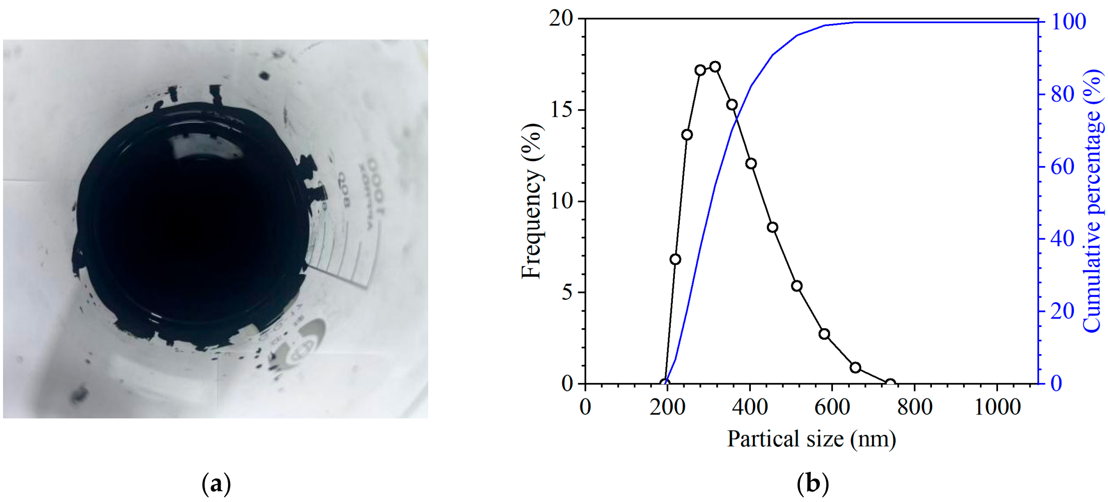

Figure 1. Nano carbon black dispersion liquid (CBDL): (**a**) NCB dispersion liquid; (**b**) Distribution of NCB.

Table 1. Properties of nano carbon black (provided by manufacturer).

Diameter (nm)	Specific Surface (m^2/g)	Pour Density (g/L)	Resistivity (Ω·cm)	DBP (mL/100 g)
15	65	170	10	190

The physical and mechanical properties of polyethylene (PE) fiber (Beijing Quantumeta Amt Co., Ltd., Beijing, China) and carbon fiber (Carbon Graphene Technology (Shenzhen) Co., Ltd., Shenzhen, China) are presented in Table 2. The carbon fiber, serving as the second carbon-based filler, has a diameter of 7 µm and a length of 3 mm, whereas the PE fiber exhibits a diameter of 24 µm and a length of 18 mm within SHCC. The tensile strain of the

PE fiber exceeds that of the carbon fiber, while the tensile strength and Young's modulus of the carbon fiber surpass those of the PE fiber.

Table 2. Properties of carbon and PE fibers.

Fiber	Diameter (μm)	Length (mm)	Density (g/cm^3)	Resistivity (Ω·cm)	Tensile Strength (MPa)	Tensile Strain (%)	Young's Modulus (GPa)
Carbon	7	3	1.75	1.2	3500	1.5	230
PE	24	18	0.97	/	3000	2.5	116

2.2. Mix Proportion

Table 3 presents the material proportions of various SHCC incorporating either a single carbon-based filler, such as NCB or carbon fiber, or a combination of both as hybrid fillers. The referenced SHCC contained 1.5 vol.% PE fibers, with a water-to-binder (cement and SF) ratio of 0.3, which was referred to [17]. These parameters were consistently maintained across the preparation of other SHCC specimens. The proportion of the first carbon-based filler, NCB, varied from 5 wt.% to 9 wt.% relative to the binder materials' weight. The volume fraction of the second carbon-based filler, carbon fiber, ranged from 0.2 vol.% to 0.6 vol.%. Hydroxypropyl methylcellulose (HPMC, with a viscosity of 200,000 cP) was incorporated to enhance the dispersion of hybrid fibers (i.e., carbon and PE fibers). Additionally, a polycarboxylate superplasticizer (SP) was employed to optimize the workability of SHCC containing hybrid fibers and hybrid carbon-based fillers (i.e., NCB and carbon fibers). It is noteworthy that the water content was adjusted when varying amounts of CBDL were introduced, where the solid content of carbon black is 20 wt.% and the polymeric dispersant is 16 wt.%. The polymeric dispersant was found to enhance the workability of the cementitious matrix, thereby eliminating the need for superplasticizers when CBDL was incorporated.

Table 3. Mix proportion of SHCC (kg/m^3) and the amount of carbon-based fillers (NCB or/and carbon fiber).

Group No.		Cement	SF	Fine Sand	Water	SP	HPMC	CBDL	NCB (wt.%)	Carbon Fiber (vol.%)	PE Fiber (vol.%)
Ref.	PE-SHCC	1000	300	390	390	2	0	0	0	0	1.5
Single carbon-based filler	CB5	1000	300	390	182	0	0	325	5	0	1.5
	CB6	1000	300	390	140	0	0	390	6	0	1.5
	CB7	1000	300	390	99	0	0	455	7	0	1.5
	CB8	1000	300	390	57	0	0	520	8	0	1.5
	CB9	1000	300	390	16	0	0	585	9	0	1.5
	CF0.2	1000	300	390	390	4	0.3	0	0	0.2	1.5
	CF0.4	1000	300	390	390	6	0.3	0	0	0.4	1.5
	CF0.6	1000	300	390	390	8	0.3	0	0	0.6	1.5
Hybrid carbon-based fillers	CB5-CF0.2	1000	300	390	182	0	0.3	325	5	0.2	1.5
	CB5-CF0.4	1000	300	390	182	0	0.3	325	5	0.4	1.5
	CB5-CF0.6	1000	300	390	182	0	0.3	325	5	0.6	1.5

Note: SF refers to silica fume, SP denotes the polycarboxylate superplasticizer, HPMC stands for hydroxypropyl methylcellulose with a viscosity of 200,000 cP, and CBDL represents the carbon black dispersion liquid. In this dispersion, the solid content of carbon black is 20 wt.%, and the polymeric dispersant constitutes 16 wt.%, as provided by the manufacturer. The percentage of NCB and chopped carbon fibers relative to the combined weight of cement and silica fume are indicated in parentheses.

2.3. Specimen Preparation

The mixing procedures for specimens containing single or hybrid carbon-based fillers are depicted in Figure 2a. A JJ-5 model cement mortar mixer (ZhongJiaoJianYi Technology

Development Co., Ltd., Beijing, China) was used, featuring low- and high-speed rotations of 140 ± 5 r/min and 285 ± 10 r/min, respectively. Initially, the binder materials, fine sand, and water were put into a mortar agitator and stirred (low-speed to high-speed) uniformly for approximately 2 min. Subsequently, the CBDL was incorporated into the fresh mortar and stirred (high-speed) for an additional 2 min. Following this, PE fibers were added, succeeded by carbon fibers. The fresh SHCC mixture was then subjected to high-speed stirring with the addition of HPMC for a minimum of 4 min. When carbon fiber served as the sole carbon-based filler, SP was also added into the mixture. The workability of the mixture was assessed using the flowability test in accordance with GB/T 2419-2005 [33]. As illustrated in Figure 2b, all fresh mixtures exhibited a comparable flowability, with a spread-flow diameter of approximately 170 mm. Finally, the fresh SHCC mixture was cast into molds of varying sizes for subsequent four-electrode voltammetry testing and mechanical testing.

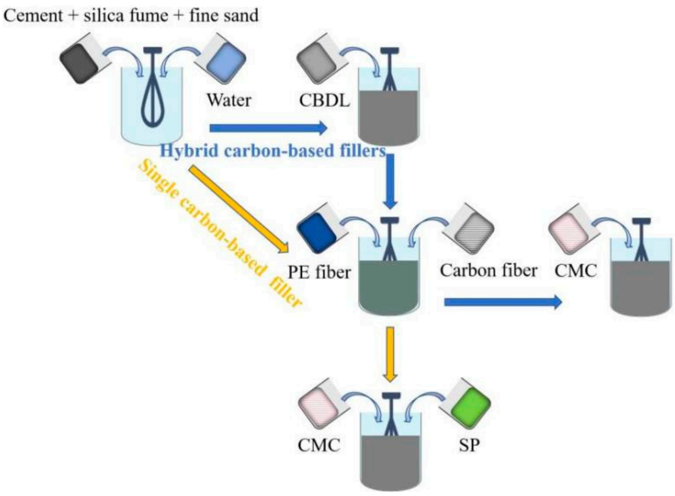

(**a**)

(**b**)

Figure 2. Preparation of SHCC mixtures: (**a**) Mixing procedures; (**b**) Flowability.

2.4. Measurement

Four-electrode voltammetry was employed to assess the electrical resistivity of all specimens. This method effectively eliminates the contact resistance between the electrode and the mortar matrix and minimizes the influence of the polarization effect [34]. The specimens measured 40 mm × 40 mm × 160 mm. A constant current of 0.1 mA was applied to the outer current electrodes, while the voltage was monitored at the inner voltage electrodes using a Gamry electrochemical workstation (Gamry Instruments, Inc., Warminster, PA, USA) [17]. The electrical resistivity testing was conducted at intervals of 7, 14, and 28 days. The electrical resistivity of the specimens was calculated using Equation (1).

$$\rho = \frac{V}{I} \times \frac{S}{L} \tag{1}$$

where ρ = electrical resistivity (Ω·m), V = measured voltage (mV), I = applied current (mA), S = contacted area between copper electrode and mortar matrix (m^2), L = spacing between inner voltage electrodes (m).

The compressive and flexural strengths of all SHCC specimens were evaluated in accordance with the GB/T17671-2021 [35]. The sample size used for the mortar strength test was a cuboid with dimensions of 40 mm × 40 mm × 160 mm in the light of the standard. The assessments were conducted using an integrated cement compressive and flexural testing machine, with specimens subjected to a curing period of 28 days. The strength test was conducted in the force control, with continuous loading until the specimen completely broke. The maximum load that the specimen could withstand was recorded to calculate the strength of SHCC. Figure 3 illustrates the uniaxial tensile tests of dumbbell-shaped SHCC specimens, conducted in this study following the Japan Society of Civil Engineers (JSCE) recommendations for design and construction of High-Performance Fiber Reinforced Cement Composites (HPFRCC) [36], also referred to as SHCC. A testing frame with a maximum capacity of 50 kN was employed, operating at a controlled displacement rate of 0.2 mm/min. Two clip-on extensometers, each with a gauge length of 80 mm, were positioned at the middle of the dumbbell-shaped SHCC to measure deformation during tensile loading. The loading was terminated when the bearing capacity of the specimen dropped below 70% of the peak load.

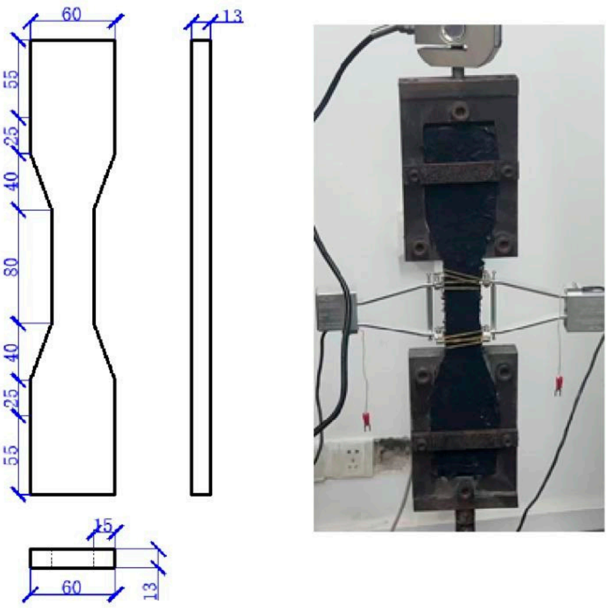

Figure 3. Uniaxial tensile testing of SHCC (unit: mm).

To study the variation in the microstructure and morphology of SHCC with single and hybrid carbon-based fillers, scanning electron microscopy (SEM, Zeiss Gemini 300, ZEISS Group, Oberkochen, Germany) was applied. Samples of the SHCC fracture surface were selected. After being dried in a 60 °C oven for 24 h, all the samples were subjected to gold spraying treatment before being observed by SEM. SEM images at different magnifications were obtained by using secondary electron mode with an accelerating voltage of 5 kV. The working distance during image acquisition ranged from 15 to 20 mm, and it was adjusted slightly according to different observation areas. The energy dispersive X-ray spectroscopy (EDS) measurement was carried out within the corresponding SEM image area. The EDS integrated with the SEM for elemental mapping analysis was employed.

3. Results and Discussion

3.1. Electrical Conductivity

Figure 4 presents the electrical resistivity of all specimens over a 28-day curing period. The electrical resistivity of PE-SHCC increased with extended curing time, indicating that the hydration reaction negatively impacts the electrical resistivity of PE-SHCC, thereby reducing its effectiveness as a conductive material. In contrast, the electrical resistivity of SHCC containing either a single carbon-based filler or hybrid carbon-based fillers significantly decreased as the amount of carbon-based fillers increased. Moreover, the rate of resistivity variation in these specimens gradually slowed or even ceased with prolonged curing durations.

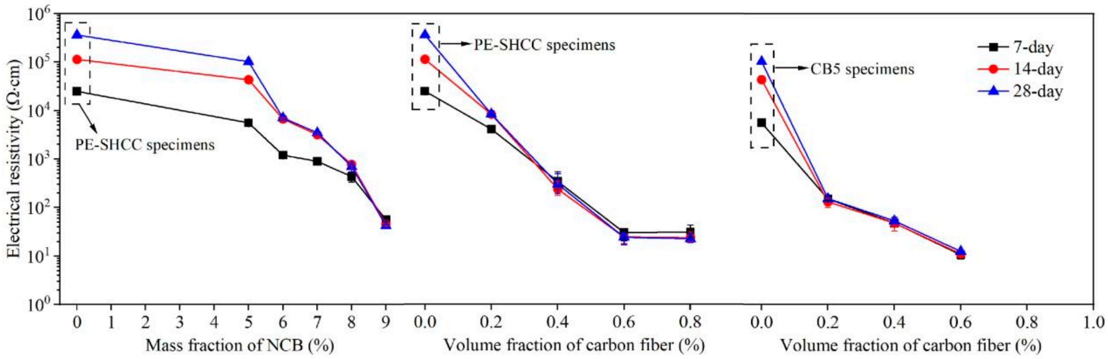

Figure 4. Effect of carbon-based fillers on the electrical resistivity of SHCC.

As reported by Zhang et al. [32], conductive pathways in cementitious composites can be classified into three categories: (i) direct contact between conductive particles, (ii) the quantum tunneling effect between conducting particles, and (iii) ion migration within the pore solution. With the progression of curing age, the hydration reaction consumes water, thereby reducing the ion migration effect. During this process, the cement reacts with water to form hydration products that occupy the pores within the cementitious matrix, which may hinder electron transport between adjacent particles and diminishes the quantum tunneling effect. Consequently, these changes in the conductive pathways contribute to an overall increase in the specimen's resistivity as the curing age advances. The electrical resistivity of SHCC remained nearly constant at 14 days and 28 days when the amount of NCB exceeded 6 wt.% or the carbon fibers exceeded 0.2 vol.%. The formation and accumulation of hydration products will gradually fill the pores, possibly exerting a physical compression and rearrangement effect on the conductive fillers dispersed in the matrix. This effect is inferred to enable the originally less closely packed conductive particles to come closer to each other more closely, thereby increasing the direct contact points, shortening the tunneling distance, and optimizing the network connectivity. When the hydration reaction is nearly complete, the microstructure of the matrix becomes relatively stable, and the "self-organization" and "compaction" effects of the conductive fillers also reach saturation. At this point, the optimization degree of the solid-state conductive network possibly reaches its maximum, and the change in electrical conductivity will tend to stabilize.

As reported by Liu et al. [37], the permeation threshold of NCB in cementitious composites is approximately 1.5% by weight of cement. Despite the CB content in CB5 exceeding this percolation threshold, its conductivity remains suboptimal. At higher content, although the number of NCB particles increases, their main function remains to fill the voids in the existing chain-like network and enhance the tunneling effect. By contrast, the carbon fiber network may have become extremely dense. The newly added carbon fibers mainly contribute to the redundancy and robustness of the network, but the marginal improvement in the overall resistivity may decrease, thereby causing the rate of resistivity change to slow down. The electrical resistivity of CB5-CF0.2 decreased by an order of magnitude compared to CF0.2 following the addition of 5 wt.% of NCB, and by three orders of magnitude compared to CB5 after the incorporation of 0.2 vol.% of carbon fiber. As the carbon fiber content increases, the resistivity decreases gradually and consistently. This phenomenon is attributed to the formation of an extensive conductive network, with the excess conductive carbon-based fillers merely occupying the interstitial spaces. The electrical resistivity of CB5-CF0.2 and CB5-CF0.4 was comparable to that of

CF0.6, where a complete conductive network was established. The design of conductive SHCC with hybrid carbon-based fillers was proposed, considering the reduced cost and the challenge of fiber agglomeration.

Conductive fillers establish conductive networks in cementitious matrix through both contact and tunneling conduction mechanisms [29,38]. As illustrated in Figure 5, NCB, being a zero-dimensional carbon material, presents challenges in forming direct contact conduction pathways. Consequently, the conductive network formed within CB5 is ineffective, resulting in unsatisfactory electrical resistivity. In contrast, carbon fiber, a one-dimensional carbon material, significantly facilitates the development of three-dimensional conductive networks in cementitious matrix. Firstly, the incorporation of carbon fiber serves a bridging function, effectively linking the conductive paths formed by the zero-dimensional NCB and enhancing contact conduction between particles. Secondly, the high electrical conductivity of carbon fiber substantially promotes the tunneling conduction of the surrounding non-contact NCB particles. Therefore, NCB and carbon fibers synergistically enhance conductivity and construct an efficient three-dimensional conductive network.

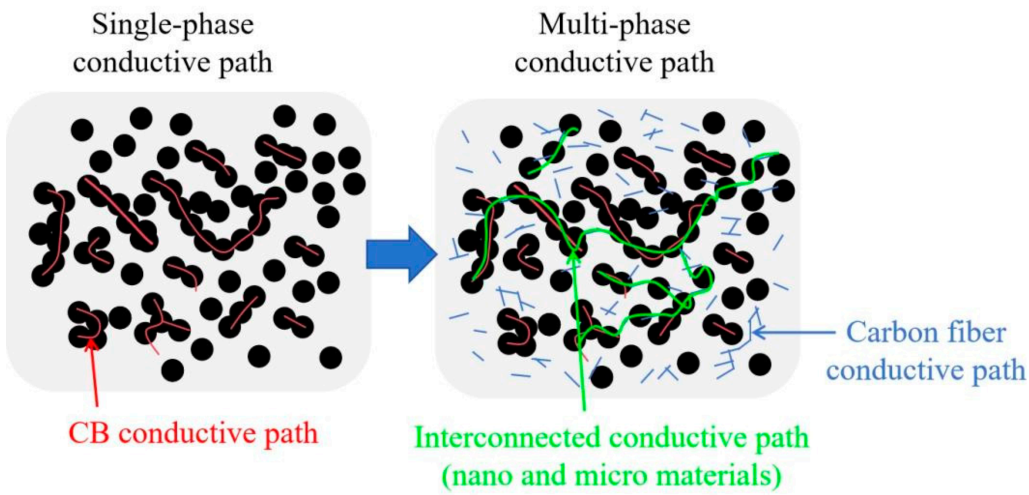

Figure 5. Single-phase vs. multi-phase conductive path in SHCC.

3.2. Compressive and Flexural Strength

Figure 6 illustrates the mechanical properties of the SHCC specimens. The compressive and flexural strengths at 28 days for specimens mixed with 5 wt.% NCB decreased by 54.3% and 27.4%, respectively, compared to the PE-SHCC specimens. This reduction in strength is likely attributable to the inherent strong tendency of NCB to agglomerate due to van der Waals forces, leading to the formation of pre-existing and further growing aggregates that act as defects [28]. The presence of a large number of aggregates disrupts the uniformity of the cement matrix, making it more brittle and reducing its ability to resist compressive and bending stresses. Nevertheless, as the NCB content increased, the mechanical properties of SHCC mixed with a single carbon-based filler exhibited minimal variation.

The compressive strength of SHCC incorporating 0.2 vol.% carbon fibers decreased from 65 MPa to 34.2 MPa, exhibiting a consistent decline with the increased amount of carbon fibers. Conversely, the flexural strength of SHCC with 0.2 vol.% carbon fibers demonstrated a slight enhancement compared to PE-SHCC. The flexural strength of SHCC with 0.4 vol.% carbon fibers decreased by 7.4%, which is significantly less than the 50.0% reduction observed in compressive strength. For the addition of 0.2 vol.% carbon fibers, the compressive strength of the specimens decreased due to the agglomeration of hybrid fibers, which promotes the formation and propagation of micro-cracks under compression. However, the flexural strength increased due to the synergistic fiber-bridging effects under tension. Similarly, an excessive amount of carbon fibers can lead to entanglement and aggregation, further exacerbating the formation of defects that may adversely affect the mechanical properties of cementitious composites [31].

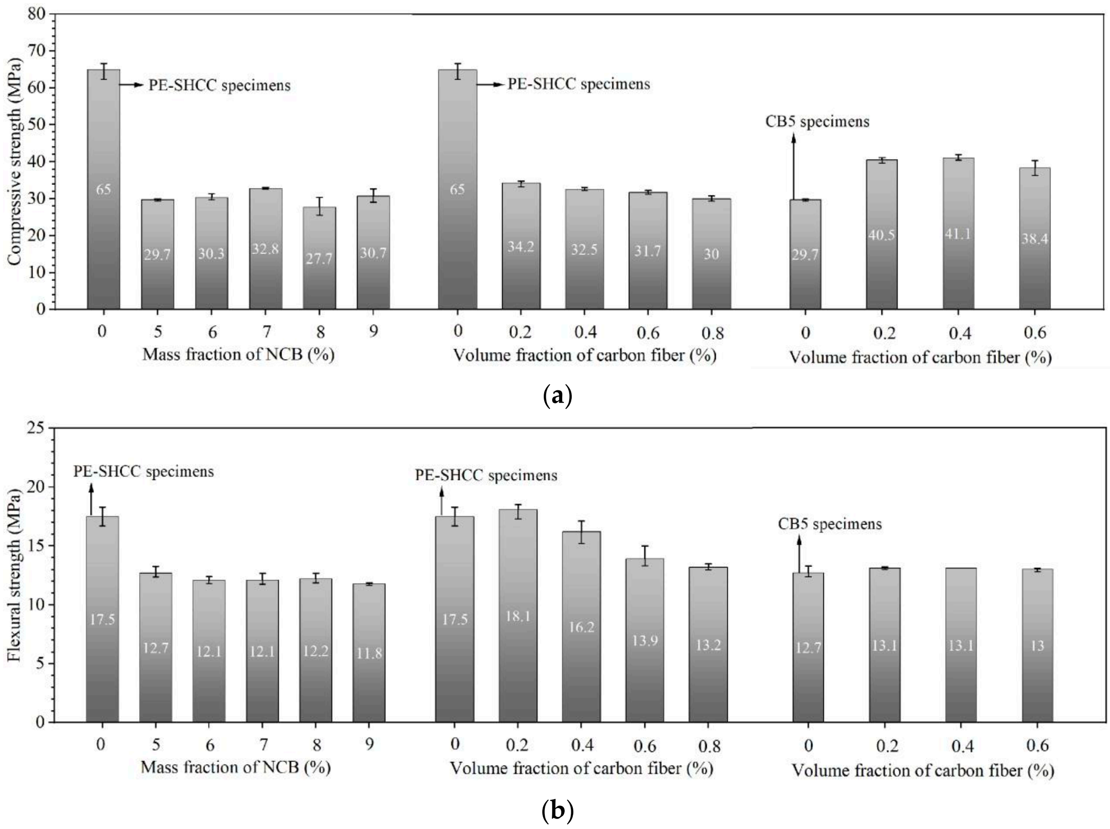

Figure 6. Effect of carbon-based fillers on the mechanical properties of SHCC: (**a**) Compressive strength; (**b**) Flexural strength.

In this study, the SHCC specimens incorporating hybrid carbon-based fillers demonstrated a positive effect on compressive strength compared to specimens with a single carbon-based filler. Specifically, for CB5-CF0.2, the compressive strength of the specimens increased by 36.4% compared to CB5 and by 18.4% compared to CF0.2 specimens. The polymeric dispersant contained in the CBDL acts by adsorbing onto the surface of NCB particles, improving the overall rheology of the mortar mixture, thereby facilitating the dispersion of NCB itself and indirectly influencing the distribution of macroscopic fibers. Hybrid fibers effectively inhibited the initiation and propagation of micro-cracks while enhancing mechanical strength under compression. However, there was negligible difference in flexural strength between CB5-CF0.2 and CB5 specimens, with a decrease observed when comparing CB5-CF0.2 to CF0.2 specimens. This may be attributed to the adverse effects of NCB agglomeration outweighing its beneficial impact on the dispersion of hybrid fibers.

3.3. Uniaxial Tensile Performance

Figure 7 illustrates the comparative observation of failure modes between PE-SHCC and SHCC incorporating hybrid carbon-based fillers under uniaxial tensile loading. All SHCC specimens exhibited multiple cracking. In the case of PE-SHCC, the distribution of multiple cracks was relatively concentrated, and failure occurred when the width of the primary crack increased abruptly. Conversely, the inclusion of carbon fibers and carbon black resulted in a more uniform distribution of multiple cracks within the testing region. To prevent single crack fracture failure and achieve multiple cracking, it is essential to ensure that the fiber-bridging strength exceeds the cracking strength of the matrix [39]. The addition of NCB reduced the cracking strength of the mortar matrix, while the incorporation of carbon fibers enhanced the fiber-bridging strength.

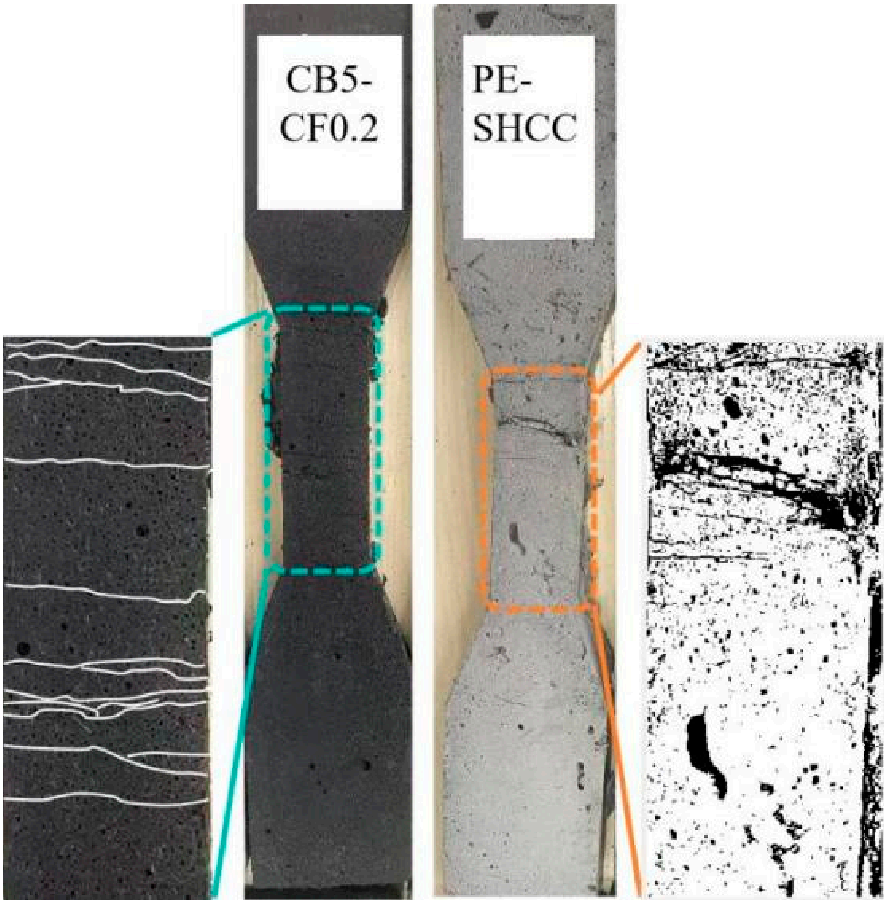

Figure 7. Comparison of tensile failure modes of SHCC.

The tensile stress–strain curves for all representative SHCC specimens are depicted in Figure 8a. An approximately bilinear tensile performance was observed across all SHCC specimens. The initial linear tensile behavior occurred prior to the onset of the first crack, during which the uncracked tensile modulus was higher. The tensile stress–strain behavior became fluctuated with the initiation and propagation of multiple cracks, resulting in a lower cracked tensile modulus. Figure 8b illustrates the effect of carbon-based fillers on the tensile strength and strain of SHCC. With the addition of NCB, the tensile strength of the specimens decreased by 23.9% to 31.7%, while the tensile strain increased by 21.3% to 60.6%. The incorporation of NCB reduced the matrix strength but enhanced the dispersion of PE fibers, thereby increasing the fiber-bridging strength. With the addition of 0.2 vol.% carbon fibers, the tensile strength of the specimens increased by 39.9%, although the magnitude of increase diminished to 19.3% as the carbon fiber content rose to 0.6 vol.%. The tensile strain of SHCC with hybrid fibers also improved compared to PE-SHCC. Upon the addition of hybrid carbon-based fillers, the tensile strength and strain of SHCC increased significantly. This is consistent with the mechanism of NCB, which reduces the friction between fibers and lowers the tendency for agglomeration [40]. The results of compression test indicate that the negative impact of the defects introduced by carbon-based fillers on the compressive strength may be greater than the positive contribution of the fiber bridging to the compression. However, for tensile properties, the effective bridging effect of the fibers can significantly counteract and even exceed the negative impact of the defects, thereby enhancing the tensile strength and strain. The tensile strength and strain of SHCC with 5 wt.% NCB and 0.2 vol.% carbon fibers were 5.81 MPa and 3.32%, respectively. The tensile strength increased to 7.41 MPa as the volume fraction of carbon fibers increased to 0.6 vol.%, while the tensile strain decreased to 1.24, which was lower than that of PE-SHCC.

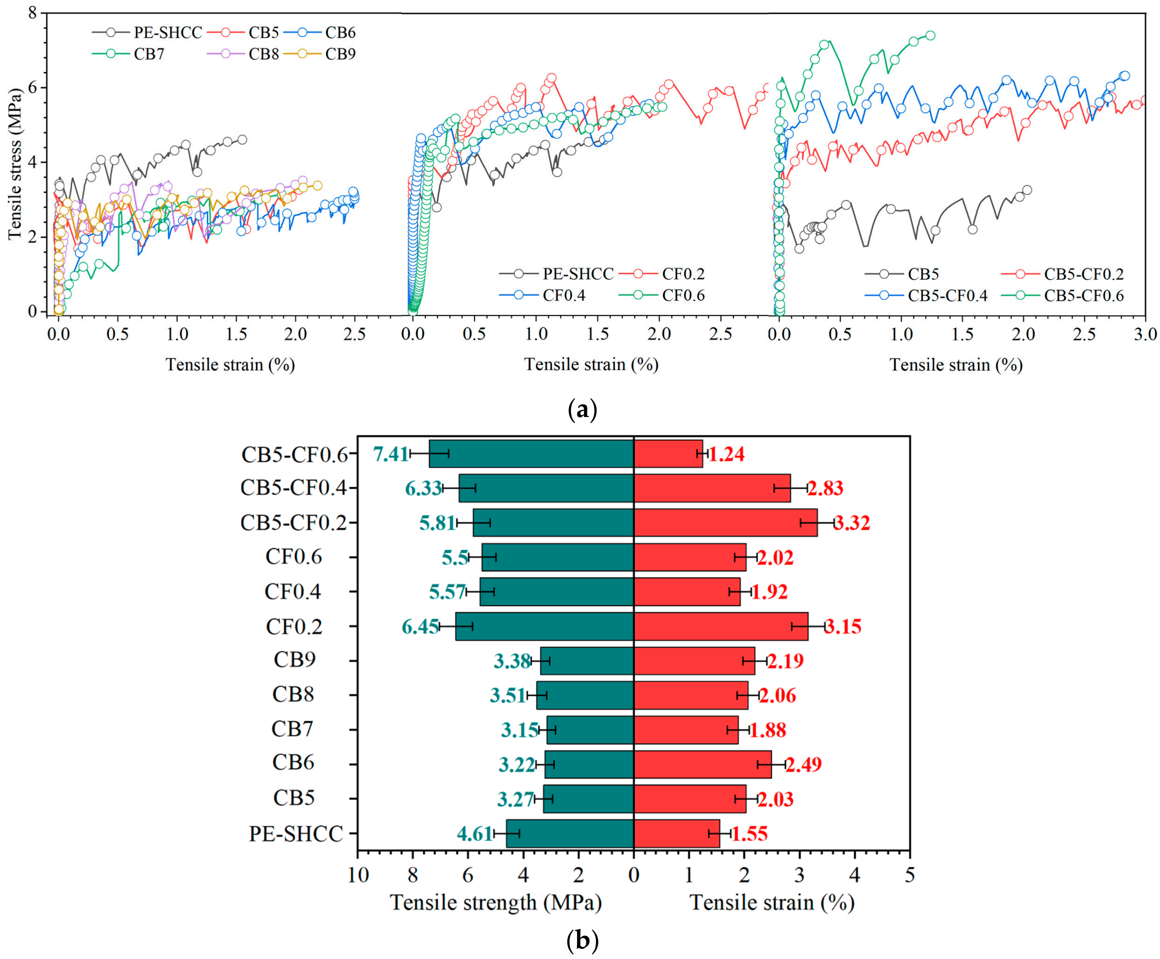

Figure 8. Effect of carbon-based fillers on the tensile behavior of SHCC: (**a**) Tensile stress–strain curves; (**b**) Tensile strength and strain.

3.4. Hybrid Efficiency Index (HEI)

The incorporation of carbon-based fillers significantly influenced both the electrical and mechanical properties of SHCC, as depicted in Figures 4, 6 and 8. Figure 9 illustrates the correlation between electrical conductivity and mechanical performance across all SHCC specimens. A reduction in both compressive and flexural strength was observed as SHCC transitioned from a non-conductive to a conductive material, attributed to the increased defects within the matrix following the addition of carbon-based fillers. The inverse relationship between electrical conductivity and compressive strength was more pronounced than that with flexural strength. Notably, the addition of hybrid carbon-based fillers enhanced the compressive strength of SHCC compared to the use of either single CB-based or carbon fiber-based fillers, as illustrated in Figure 9a. Furthermore, a significant positive correlation between electrical conductivity and tensile strength was observed with the adoption of hybrid carbon-based fillers, as shown in Figure 9c. As electrical conductivity increased, the tensile strength of SHCC exhibited a gradual increase.

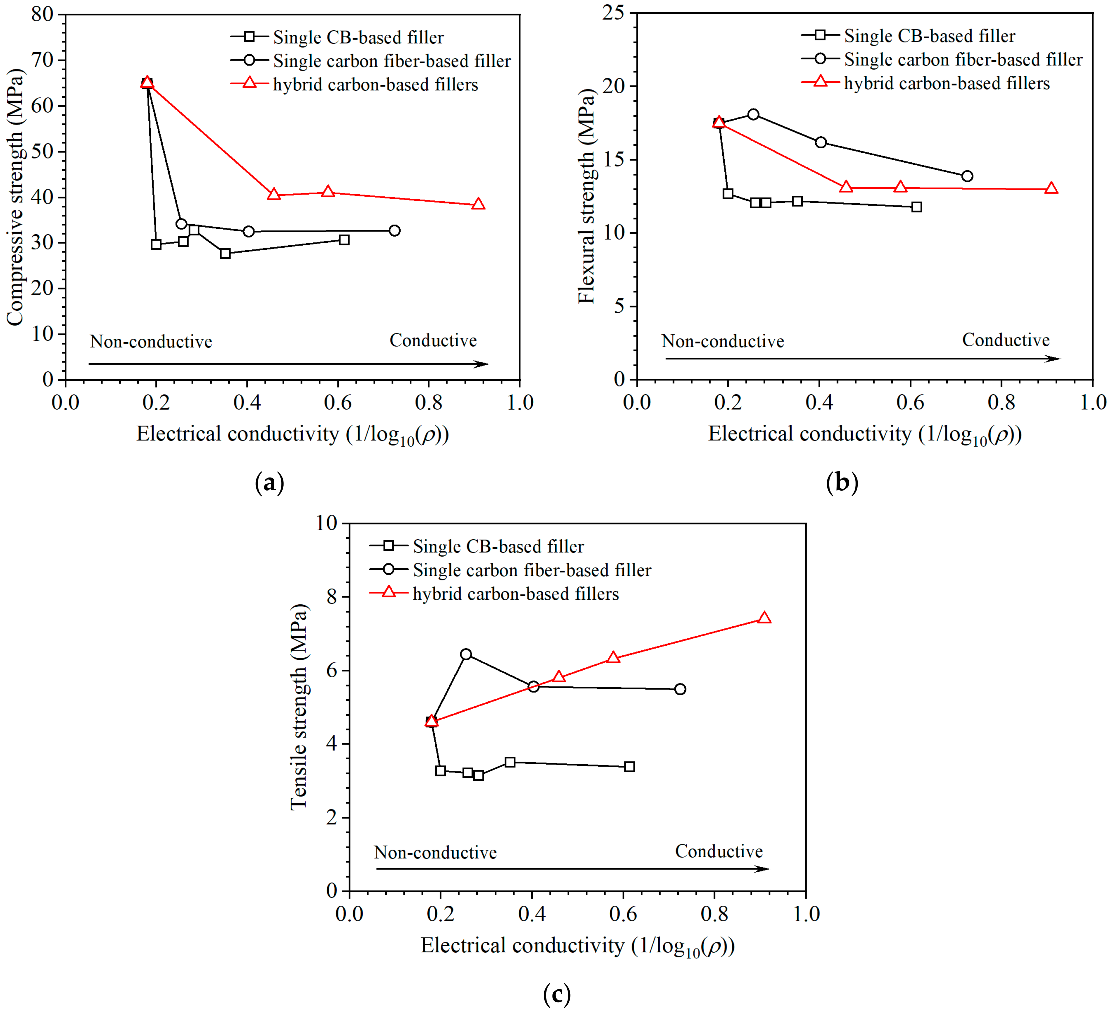

Figure 9. Correlation between electrical conductivity and mechanical properties: (**a**) Compressive strength; (**b**) Flexural strength; (**c**) Tensile strength.

When utilizing SHCC as multifunctional materials, it is imperative to concurrently consider both electrical and mechanical performance. This study introduced a hybrid efficiency index (HEI) to assess these performances when single or hybrid carbon-based fillers were incorporated into PE-SHCC. The HEI is determined using Equations (2)–(5), which involves nondimensionalization and normalization processes. A weight adjustment coefficient (α and β) was employed to prioritize either property based on specific application requirements, such as emphasizing electrical conductivity or mechanical properties. For instance, if electrical conductivity is prioritized, α = 0.4 and β = 0.6 may be selected. If both properties are equally significant, α = 0.5 and β = 0.5 should be used. The larger the HEI value, the higher the efficiency.

$$\text{HEI} = \alpha\frac{\Delta\sigma}{\sigma_0} - \beta\frac{\Delta\rho}{\rho_0} \quad (2)$$

$$\Delta\sigma = \sigma - \sigma_0 \quad (3)$$

$$\Delta\rho = \rho - \rho_0 \quad (4)$$

$$\alpha + \beta = 1 \quad (5)$$

where σ and ρ = mechanical properties (i.e., compressive, flexural and tensile strength) and electrical resistivity of SHCC with carbon-based filler additives, σ_0 and ρ_0 = mechanical properties and electrical resistivity of referenced PE-SHCC, $\Delta\sigma$ = variation of strength, $\Delta\rho$ = variation of electrical resistivity (usually negative value), α and β = weight coefficient of strength and electrical resistivity.

Figure 10 illustrates the HEI values when single or hybrid carbon-based fillers were incorporated into PE-SHCC. A sensitivity analysis was performed by adjusting the weight coefficients (α and β) to examine the impact of weight variations on the HEI outcomes. A negative HEI value was observed when the emphasis on mechanical properties exceeded that of electrical conductivity, particularly with the addition of single CB-based filler. The compressive strength demonstrated greater sensitivity to the inclusion of carbon black, followed by the flexural and tensile strengths of SHCC. The HEI was notably positive when hybrid carbon-based fillers were introduced into PE-SHCC, especially concerning electrical conductivity and tensile strength. The combination of these variables is designed to comprehensively evaluate the overall performance of SHCC as a multifunctional material in terms of electrical properties and the main mechanical properties (compression, flexure, tension). The HEI value gradually increased as the focus shifted from mechanical properties to electrical conductivity. Compared to tensile strength, the HEI was more sensitive to changes in compressive and flexural strengths. A higher HEI value indicated a reduced negative impact of carbon-based fillers on mechanical properties while enhancing electrical conductivity. In the case of hybrid carbon-based fillers, this may even result in an enhancement effect, indicating a higher improvement efficiency. When focusing on mechanical properties, for instance α = 0.7 and β = 0.3 or α = 0.6 and β = 0.4, the HEI value of CB5-CF0.2 was significantly higher than that of others, demonstrating its advantage in enhancing compressive, flexural and tensile strength. When focusing on electrical properties, for instance α = 0.3 and β = 0.7 or α = 0.4 and β = 0.6, the combination of 5 wt.% NCB and 0.6 vol.% carbon fibers can most effectively balance the significant improvement in electrical performance with the maintenance of mechanical properties, demonstrating the best overall efficiency.

It should be noted that HEI balances the priority of mechanical properties and electrical conductivity using weight coefficients α and β, yet their setting relies heavily on specific application requirements and designers' subjective judgment. As a relative index, HEI assesses efficiency by comparing the performance of carbon-based filler-modified SHCC against the reference (PE-SHCC)—its numerical value and interpretation of "efficiency" are thus highly dependent on the selected reference material. Furthermore, as a macroscopic index, HEI may fail to precisely capture the complex microscopic physicochemical interactions and the resulting nonlinear performance variations.

3.5. Microscopic Observation

Figure 11 illustrates the morphology of the fracture surface of PE-SHCC, SHCC with a single carbon-based filler, and SHCC with hybrid carbon-based fillers. The carbon fibers depicted in Figure 11a exhibit a high length-to-diameter ratio, thereby establishing macroscopic conductive pathways within the cementitious matrix. Figure 11b presents the distribution of conductive fillers of NCB particles. The distribution of CB particles in the mortar matrix was reflected by EDS mapping image of carbon element (Figure 11c). According to the micromorphology and the carbon content, the enriching CB particles were attached on the PE fibers and around the hydration products in the way of agglomeration. Figure 11d demonstrates the synergistic interaction between carbon fibers and NCB. NCB typically appears as aggregates in cementitious matrix due to van der Waals forces. The NCB aggregates surrounding the carbon fibers are distributed relatively uniformly, as shown in Figure 11d,e. Compared with the obvious agglomeration of NCB as shown in Figure 11b, the coexistence of carbon fibers and NCB in the hybrid system seems to facilitate the distribution of NCB around the fibers and indirectly supports the positive effect of NCB on the dispersion of the fibers. The presence of numerous spherical structures within the matrix forms a chain-like conductive path through contact and tunneling effects. The high aspect ratio of carbon fibers effectively connects the NCB aggregates, transforming the original chain-like conductive path of NCB aggregates into a three-dimensional conductive network, thereby enhancing the integrity and efficacy of the conductive network. Ou et al. [28] also reported similar phenomenon. However, agglomeration of NCB was observed in both cases (Figure 11b,d), which may adversely affect the mechanical strength of the cementitious composites.

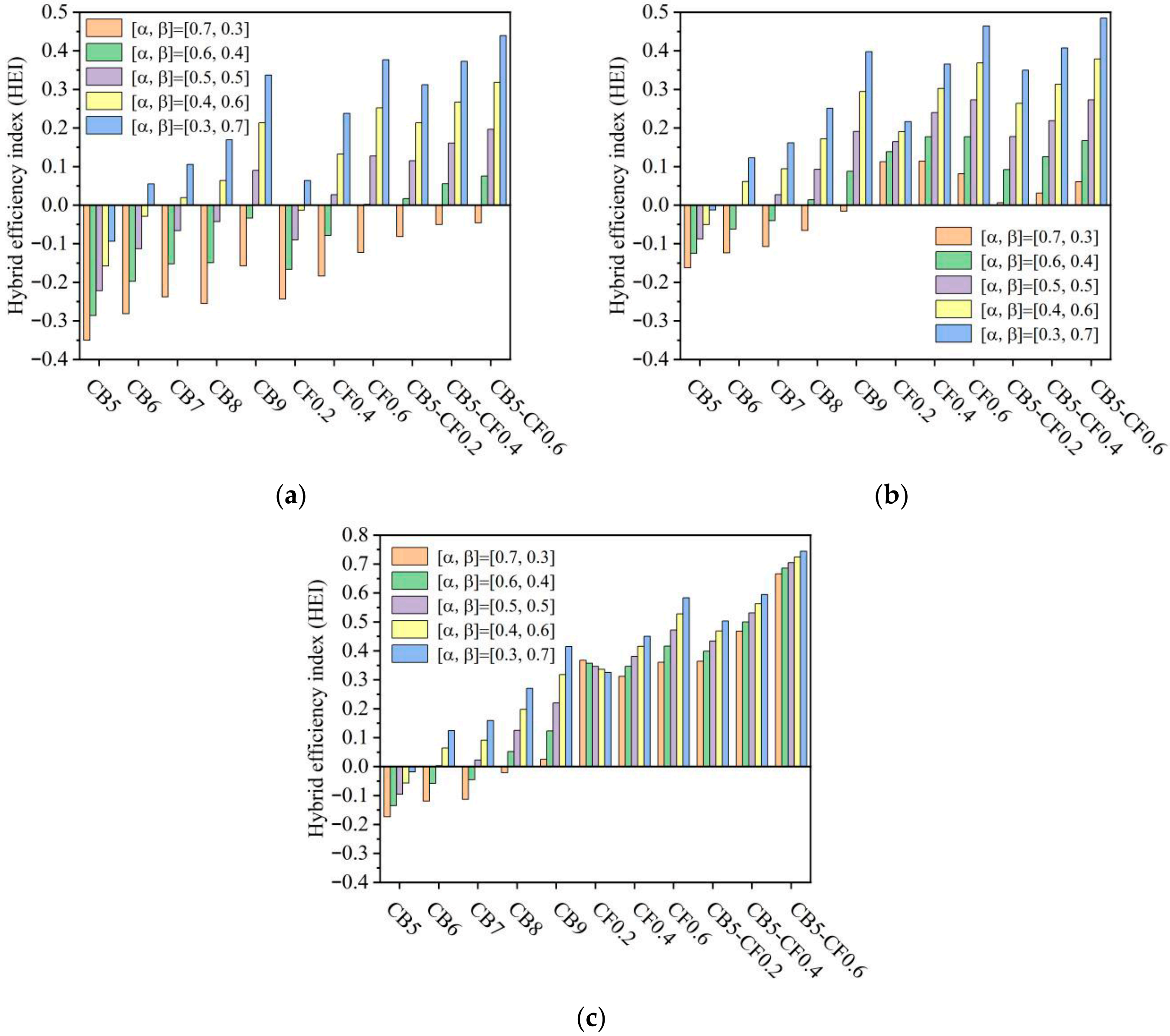

Figure 10. Hybrid efficiency index of SHCC: (**a**) Compressive strength; (**b**) Flexural strength; (**c**) Tensile strength.

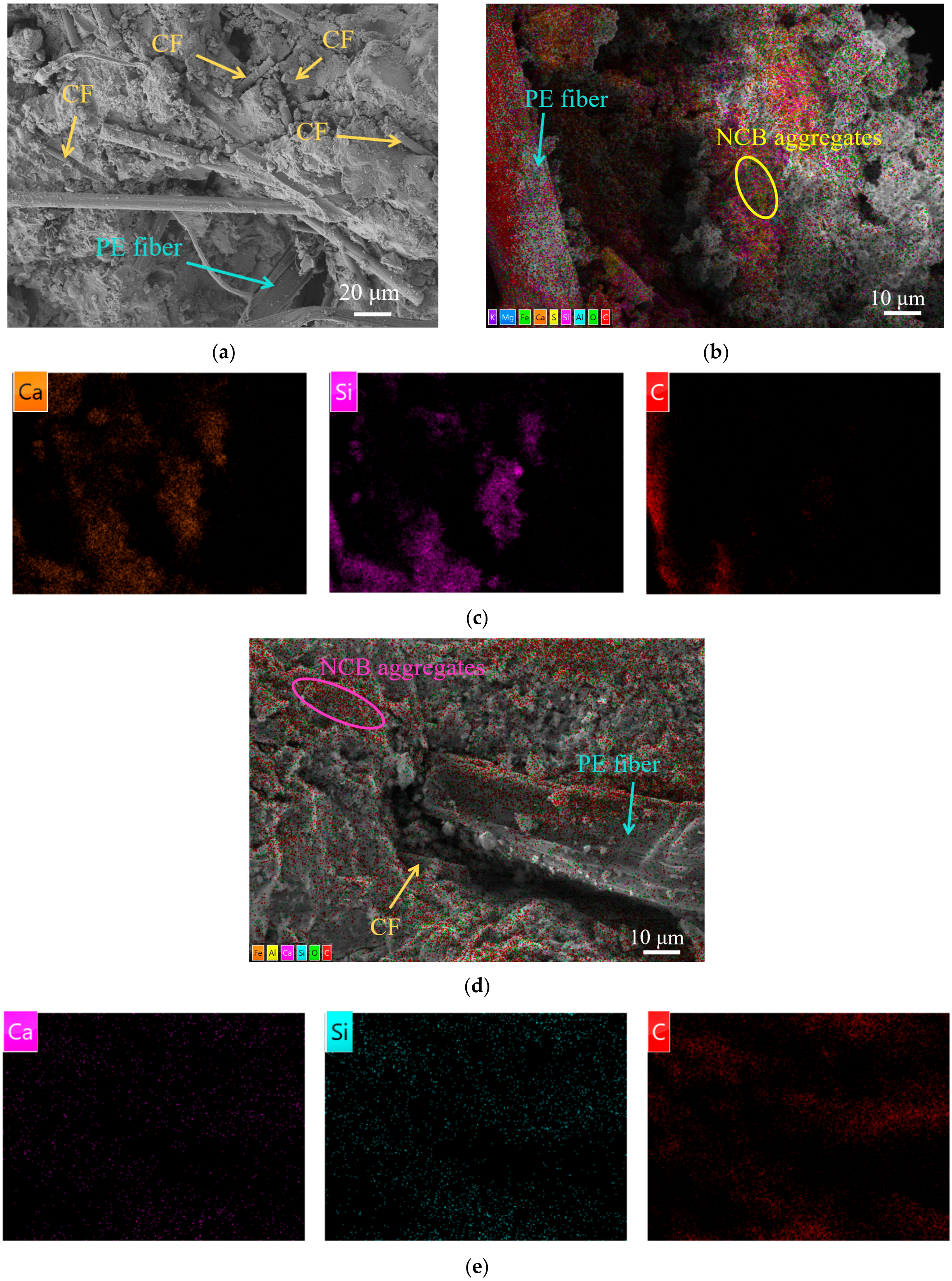

Figure 11. Effect of carbon-based fillers on the microscopic structures of SHCC: (**a**) CF0.2; (**b**) EDS mapping of CB5; (**c**) Element mapping of CB5; (**d**) EDS mapping of CB5-CF0.2; (**e**) Element mapping.

4. Conclusions

The following findings and conclusions can be drawn from this study:

(1) The electrical resistivity of SHCC with either single or hybrid carbon-based fillers decreases significantly with increasing filler content. Specifically, integrating 5 wt.% NCB and 0.2 vol.% carbon fibers reduces the electrical resistivity of PE-SHCC by three orders of magnitude, lowering it to <150 Ω·cm.
(2) Adding carbon black to PE-SHCC reduces both compressive and flexural strength, due to NCB particle aggregation. Conversely, incorporating 0.2 vol.% carbon fiber decreases compressive strength but enhances flexural strength. Furthermore, adding 5 wt.% NCB to the 0.2 vol.% carbon fiber-reinforced PE-SHCC increases compressive strength by 18.4%.
(3) Carbon black incorporation in PE-SHCC reduces tensile strength while improving ductility. Conversely, carbon fiber enhances PE-SHCC's tensile properties; however, this improvement diminishes with excessive carbon fiber. Optimal tensile strength (5.81 MPa) and tensile strain (3.32%) are achieved by adding 5 wt.% NCB and 0.2 vol.% carbon fiber to PE-SHCC.
(4) A hybrid efficiency index (HEI) is proposed for comprehensively evaluating the trade-offs and synergistic effects between electrical conductivity and various mechanical properties in multifunctional cementitious composites, particularly under different weighting priorities (α and β). This offers a new methodology for future material design.

It should be noted that the long-term performance and durability of these hybrid SHCC, including electrical stability, mechanical degradation, and resistance to environmental factors, have not been thoroughly explored. Investigating the sustained electrical/mechanical performance and self-sensing capabilities of these materials under prolonged service conditions and diverse environmental exposures (e.g., freeze–thaw cycles, wetting-drying, sustained loading) is crucial for practical engineering applications. Additionally, this study focused on a defined range of filler contents and a fixed PE fiber volume fraction. It is acknowledged that the optimal hybrid efficiency achieved is specific to the tested proportions and may vary with different matrix designs or fiber types. Furthermore, employing advanced characterization techniques (e.g., X-ray computed tomography) to quantitatively analyze 3D conductive network formation, filler dispersion, and fiber-matrix interfaces across multiple scales would offer deeper understanding of the synergistic mechanisms.

Author Contributions: Conceptualization, L.W. and Y.Z.; methodology, L.W., C.X. and B.Y.; investigation, C.X. and B.Y.; data curation, C.X.; writing—original draft preparation, L.W.; writing—review and editing, L.W., B.Y., S.H. and Y.Z.; supervision, L.W. and Y.Z.; project administration, L.W.; funding acquisition, L.W., S.H. and Y.Z. All authors have read and agreed to the published version of the manuscript.

Funding: This research was funded by the National Natural Science Foundation of China (52208183), the Regional Joint Project for Foundation and Applied Basic Research of Guangdong Province (2021A1515110292), the Science and Technology Development Fund (0101/2024/AMJ), the National Key Research and Development Program of China (2024FE0201900), the Natural Science Foundation of Guangdong Province (2025A1515010864).

Data Availability Statement: The original contributions presented in the study are included in the article, further inquiries can be directed to the corresponding author.

Conflicts of Interest: The authors declare no conflicts of interest.

Abbreviations

The following abbreviations are used in this manuscript:

SHCCs	Strain-hardening cementitious composites
PE	Polyethylene
CF	Carbon fiber
CB	Carbon black
NCB	Nano carbon black
CBDL	Nano carbon black dispersion liquid
HyFRCC	Hybrid fiber reinforced cementitious composites
HEI	hybrid efficiency index HEI

References

1. Pei, C.; Wei, L.; Qin, Z.; Yu, H.; Zhu, J.H.; Xing, F. Behavior and design of nano/micro-scale carbon modified multifunctional cementitious composites. *Constr. Build. Mater.* **2022**, *314*, 125506. [CrossRef]
2. Li, W.; Dong, W.; Guo, Y.; Wang, K.; Shah, S.P. Advances in multifunctional cementitious composites with conductive carbon nanomaterials for smart infrastructure. *Cem. Concr. Compos.* **2022**, *128*, 104454. [CrossRef]
3. Li, V.C. High-performance and multifunctional cement-based composite material. *Engineering* **2019**, *5*, 250–260. [CrossRef]
4. Ran, H.; Elchalakani, M.; Liu, H.; Yehia, S.; Yang, B. Development and characteristics of multifunctional ultra-lightweight engineered cementitious composites incorporating cenospheres and PE fibre. *Cem. Concr. Compos.* **2023**, *140*, 105084. [CrossRef]
5. Zhong, S.; Yuan, S.; Zhang, X.; Zhang, J.; Xu, L.; Xu, T.; Zuo, T.; Cai, Y.; Yi, L. Hierarchical cellulose aerogel reinforced with in situ-assembled cellulose nanofibers for building cooling. *ACS Appl. Mater. Interfaces.* **2023**, *15*, 39807–39817. [CrossRef]
6. Calvino, M.M.; Lisuzzo, L.; Cavallaro, G.; Lazzara, G.; Milioto, S. Halloysite based geopolymers filled with wax microparticles as sustainable building materials with enhanced thermo-mechanical performances. *J. Environ. Chem. Eng.* **2022**, *10*, 108594. [CrossRef]
7. Li, D.; Tang, Y.; Zuo, X.; Zhao, X.; Zhang, X.; Yang, H. Preparation of hierarchical porous microspheres composite phase change material for thermal energy storage concrete in buildings. *Appl. Clay. Sci.* **2023**, *232*, 106771. [CrossRef]
8. Jin, P.; Kohestanian, M.; Hasany, M.; Akhiani, A.R.; Su, Y.; Mehrali, M. Multifunctional Cement-Based Composite with Advanced Self-Sensing, Electrothermal, and Electrochemical Properties. *Adv. Funct. Mater.* **2025**, *35*, 2411878. [CrossRef]
9. Pang, C.; Pei, H.; Li, Z. Performance investigation of cement-based laminated multifunctional magnetoelectric composites. *Constr. Build. Mater.* **2017**, *134*, 585–593. [CrossRef]
10. Pisello, A.L.; D'Alessandro, A.; Sambuco, S.; Rallini, M.; Ubertini, F.; Asdrubali, F.; Materazzi, A.L.; Cotana, F. Multipurpose experimental characterization of smart nanocomposite cement-based materials for thermal-energy efficiency and strain-sensing capability. *Sol. Energy Mater. Sol. Cells* **2017**, *161*, 77–88. [CrossRef]
11. Górski, M.; Safuta, M. Functional carbon-based materials for structural health monitoring and protection of concrete structures. *Struct. Concr.* **2025**, *26*, 5370–5390. [CrossRef]
12. Gao, X.; Li, W.; Wang, P.; Lu, Y.; Zhou, J.; Wang, X.Q. Advancing energy solutions: Carbon-based cementitious composites in energy storage and harvesting. *J. Build. Eng.* **2024**, *91*, 109720. [CrossRef]
13. Huang, B.T.; Zhu, J.X.; Weng, K.F.; Li, V.C.; Dai, J.G. Ultra-high-strength engineered/strain-hardening cementitious composites (ECC/SHCC): Material design and effect of fiber hybridization. *Cem. Concr. Compos.* **2022**, *129*, 104464. [CrossRef]
14. Wei, L.; Zheng, Y.; Tian, J.; Wu, X.; Shen, H.; Zhu, J.H. Investigation into the fracture mechanical performance of strain hardening cementitious composites hybridized with polyethylene and carbon fiber using digital image correlation (DIC) technique. *Structures* **2025**, *78*, 109339. [CrossRef]
15. Tian, J.; Zhu, W.; Wu, X.; Sun, C.; Zheng, Y.; Tang, S.; Yuan, J.; Zuo, Y. Deterioration test and damage model of FRP-ECC-concrete composite interface under sulfate-dry-wet cycles. *Constr. Build. Mater.* **2025**, *471*, 140723. [CrossRef]
16. Lu, Z.; Yin, R.; Yao, J.; Leung, C.K. Surface modification of polyethylene fiber by ozonation and its influence on the mechanical properties of Strain-Hardening Cementitious Composites. *Compos. Part B-Eng.* **2019**, *177*, 107446. [CrossRef]
17. Zhu, J.H.; Shen, H.; Wei, L. A study on HyFRCC consisting of PE and carbon fiber: Investigation of electrical and fracture properties based on orthogonal design. *Struct. Concr.* **2024**, *25*, 1018–1030. [CrossRef]
18. Tian, J.; Wu, X.; Tan, X.; Zuo, Y.; Zheng, Y.; Yuan, J.; Wang, W.W.; Wei, L.; Zhang, W. Feasibility study of smart functional strain-hardening cementitious composites: Self-sensing model and experimental performance. *Constr. Build. Mater.* **2024**, *436*, 136850. [CrossRef]
19. Dong, W.; Li, W.; Guo, Y.; He, X.; Sheng, D. Effects of silica fume on physicochemical properties and piezoresistivity of intelligent carbon black-cementitious composites. *Constr. Build. Mater.* **2020**, *259*, 120399. [CrossRef]
20. Lu, D.; Leng, Z.; Lu, G.; Wang, D.; Huo, Y. A critical review of carbon materials engineered electrically conductive cement concrete and its potential applications. *Int. J. Smart Nano Mater.* **2023**, *14*, 189–215. [CrossRef]

21. Dinesh, A.; Saravanakumar, P.; Prasad, B.R.; Raj, S.K. Carbon black based self-sensing cement composite for structural health monitoring–A review on strength and conductive characteristics. *Mater. Today Proc.* **2023**. [CrossRef]
22. Chen, B.; Wu, K.; Yao, W. Conductivity of carbon fiber reinforced cement-based composites. *Cem. Concr. Compos.* **2004**, *26*, 291–297. [CrossRef]
23. Tao, J.; Wang, J.; Zeng, Q. A comparative study on the influences of CNT and GNP on the piezoresistivity of cement composites. *Mater. Lett.* **2020**, *259*, 126858. [CrossRef]
24. Gao, J.; Wang, Z.; Zhang, T.; Zhou, L. Dispersion of carbon fibers in cement-based composites with different mixing methods. *Constr. Build. Mater.* **2017**, *134*, 220–227. [CrossRef]
25. Wu, S.; Mo, L.; Shui, Z.; Chen, Z. Investigation of the conductivity of asphalt concrete containing conductive fillers. *Carbon* **2005**, *43*, 1358–1363. [CrossRef]
26. Xie, P.; Gu, P.; Beaudoin, J.J. Electrical percolation phenomena in cement composites containing conductive fibres. *J. Mater. Sci.* **1996**, *31*, 4093–4097. [CrossRef]
27. Gwon, S.; Kim, H.; Shin, M. Self-heating characteristics of electrically conductive cement composites with carbon black and carbon fiber. *Cem. Concr. Compos.* **2023**, *137*, 104942. [CrossRef]
28. Ou, X.; Ye, G.; Jiang, J.; Gong, J.; He, Z. Improving electrical and mechanical properties of cement composites by combined addition of carbon black and carbon nanotubes and steel fibers. *Constr. Build. Mater.* **2024**, *438*, 136931. [CrossRef]
29. Li, M.; Gao, P.; Li, G.; Zhao, Z.; Zhang, Q.; Zhang, J.; Xu, X. Fabrication and electrical properties of carbon fiber, graphite and nano carbon black conductive cement-based composites. *Case Stud. Therm. Eng.* **2024**, *60*, 104834. [CrossRef]
30. Nalon, G.H.; Ribeiro, J.C.; de Araújo, E.N.; Pedroti, L.G.; de Carvalho, J.M.; Santos, R.F.; Aparecido-Ferreira, A. Effects of different kinds of carbon black nanoparticles on the piezoresistive and mechanical properties of cement-based composites. *J. Build. Eng.* **2020**, *32*, 101724. [CrossRef]
31. Zhu, H.; Zhou, H.; Gou, H. Evaluation of carbon fiber dispersion in cement-based materials using mechanical properties, conductivity, mass variation coefficient, and microstructure. *Constr. Build. Mater.* **2021**, *266*, 120891. [CrossRef]
32. Zhang, Q.; Luan, C.; Yu, C.; Huang, Y.; Zhou, Z. Mechanisms of carbon black in multifunctional cement matrix: Hydration and microstructure perspectives. *Constr. Build. Mater.* **2022**, *346*, 128455. [CrossRef]
33. *GB/T 2419-2005*; Test Method for Fluidity of Cement Mortar. National Standard of the People's Republic of China: Beijing, China, 2005.
34. Han, B.; Guan, X.; Ou, J. Electrode design, measuring method and data acquisition system of carbon fiber cement paste piezoresistive sensors. *Sens. Actuators A Phys.* **2007**, *135*, 360–369. [CrossRef]
35. *GB/T17671-2021*; Test Method of Cement Mortar Strength. National Standard of the People's Republic of China: Beijing, China, 2021.
36. JSCE. *Recommendations for Design and Construction of High Performance Fiber Reinforced Cement Composite with Multiple Fine Cracks*; Concrete Engineering Series 82; Japan Society of Civil Engineers: Tokyo, Japan, 2008.
37. Liu, L.; Xu, J.; Yin, T.; Wang, Y.; Chu, H. Improving electrical and piezoresistive properties of cement-based composites by combined addition of nano carbon black and nickel nanofiber. *J. Build. Eng.* **2022**, *51*, 104312. [CrossRef]
38. Qin, H.; Ding, S.; Ashour, A.; Zheng, Q.; Han, B. Revolutionizing infrastructure: The evolving landscape of electricity-based multifunctional concrete from concept to practice. *Prog. Mater. Sci.* **2024**, *145*, 101310. [CrossRef]
39. Li, V.C. *Engineered Cementitious Composites (ECC): Bendable Concrete for Sustainable and Resilient Infrastructure*; Springer: Berlin/Heidelberg, Germany, 2019.
40. Li, W.; Dong, W.; Shen, L.; Castel, A.; Shah, S.P. Conductivity and piezoresistivity of nano-carbon black (NCB) enhanced functional cement-based sensors using polypropylene fibres. *Mater. Lett.* **2020**, *270*, 127736. [CrossRef]

https://doi.org/10.3390/buildings16020267